UNIVERSITY OF BIRMINGHAM
University of Birmingham Research at Birmingham

Characterization of products formed from the oxidation of toluene and m-xylene with varying NO_x and OH exposure

Srivastava, Deepchandra; Li, Weiran; Tong, Shengrui; Shi, Zongbo; Harrison, Roy M.

DOI:
10.1016/j.chemosphere.2023.139002

License:
Creative Commons: Attribution (CC BY)

Document Version
Publisher's PDF, also known as Version of record

Citation for published version (Harvard):
Srivastava, D, Li, W, Tong, S, Shi, Z & Harrison, RM 2023, 'Characterization of products formed from the oxidation of toluene and m-xylene with varying NO_x and OH exposure', *Chemosphere*, vol. 334, 139002. https://doi.org/10.1016/j.chemosphere.2023.139002

Link to publication on Research at Birmingham portal

General rights
Unless a licence is specified above, all rights (including copyright and moral rights) in this document are retained by the authors and/or the copyright holders. The express permission of the copyright holder must be obtained for any use of this material other than for purposes permitted by law.

•Users may freely distribute the URL that is used to identify this publication.
•Users may download and/or print one copy of the publication from the University of Birmingham research portal for the purpose of private study or non-commercial research.
•User may use extracts from the document in line with the concept of 'fair dealing' under the Copyright, Designs and Patents Act 1988 (?)
•Users may not further distribute the material nor use it for the purposes of commercial gain.

Where a licence is displayed above, please note the terms and conditions of the licence govern your use of this document.

When citing, please reference the published version.

Take down policy
While the University of Birmingham exercises care and attention in making items available there are rare occasions when an item has been uploaded in error or has been deemed to be commercially or otherwise sensitive.

If you believe that this is the case for this document, please contact UBIRA@lists.bham.ac.uk providing details and we will remove access to the work immediately and investigate.

Download date: 30. Apr. 2024

Chemosphere 334 (2023) 139002

Contents lists available at ScienceDirect

Chemosphere

journal homepage: www.elsevier.com/locate/chemosphere

Characterization of products formed from the oxidation of toluene and *m*-xylene with varying NO_x and OH exposure

Deepchandra Srivastava [a], Weiran Li [b], Shengrui Tong [b], Zongbo Shi [a], Roy M. Harrison [a,1,*]

[a] School of Geography, Earth & Environmental Sciences, University of Birmingham, Birmingham, B15 2TT, United Kingdom
[b] State Key Laboratory for Structural Chemistry of Unstable and Stable Species, CAS Research/Education Center for Excellence in Molecular Sciences, Institute of Chemistry, Chinese Academy of Sciences, Beijing 100190, China

HIGHLIGHTS

- PAM chamber was used to investigate the oxidised products from *m*-xylene and toluene.
- Filter samples were analysed using GC × GC-TOFMS.
- High number of ring-opening compounds were observed from toluene oxidation.
- SOA yields were higher for both precursors under high-NO_x than at low-NO_x.
- DHOPA (2,3-dihydroxy-4-oxo-pentanoic acid), was observed in both oxidation systems.

GRAPHICAL ABSTRACT

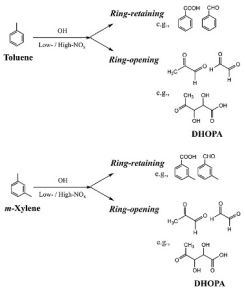

ARTICLE INFO

Handling Editor: Volker Matthias

Keywords:
Oxidation
Toluene
m-Xylene
OH radicals
SOA yields

ABSTRACT

Aromatic volatile organic compounds (VOCs) are an important precursor of secondary organic aerosol (SOA) in the urban environment. SOA formed from the oxidation of anthropogenic VOCs can be substantially more abundant than biogenic SOA and has been shown to account for a significant fraction of fine particulate matter in urban areas. A potential aerosol mass (PAM) chamber was used to investigate the oxidised products from the photo-oxidation of *m*-xylene and toluene. The experiments were carried out with OH radical as oxidant in both high- and low-NO_x conditions and the resultant aerosol samples were collected using quartz filters and analysed by GC × GC-TOFMS. Results show the oxidation products derived from both precursors included ring-retaining and -opening compounds (unsaturated aldehydes, unsaturated ketones and organic acids) with a high number of ring-opening compounds observed from toluene oxidation. Glyoxal and methyl glyoxal were the major ring-cleavage products from both oxidation systems, indicating that a bicyclic route plays an important role in their formation. SOA yields were higher for both precursors under high-NO_x (toluene: 0.111; *m*-xylene: 0.124) than at low-NO_x (toluene: 0.089; *m*-xylene: 0.052), likely linked to higher OH concentrations during low-NO_x experiments which may lead to higher degree of fragmentation. DHOPA (2,3-dihydroxy-4-oxo-pentanoic acid), a known tracer of toluene oxidation, was observed in both oxidation systems. The mass fraction of DHOPA in SOA from toluene oxidation was about double the value reported previously, but it should not be regarded as a tracer solely for oxidation of toluene as *m*-xylene oxidation gave a similar relative yield.

* Corresponding author.
E-mail address: r.m.harrison@bham.ac.uk (R.M. Harrison).
[1] Also at: Department of Environment, Faculty of Environmental Sciences, King Abdulaziz University, Jeddah, 21589, Saudi Arabia.

https://doi.org/10.1016/j.chemosphere.2023.139002
Received 24 November 2022; Received in revised form 16 May 2023; Accepted 20 May 2023
Available online 21 May 2023
0045-6535/© 2023 The Authors. Published by Elsevier Ltd. This is an open access article under the CC BY license (http://creativecommons.org/licenses/by/4.0/).

1. Introduction

Secondary organic aerosols (SOA) are formed via the atmospheric oxidation of volatile and semi-volatile organic compounds (VOCs) (Hunter et al., 2014; Srivastava et al., 2022). The formation of SOA has recently received much attention because of its possible impacts on the radiative balance (climate change), visibility degradation, and health effects of particulate matter (Daellenbach et al., 2020; Srivastava et al., 2022). Aromatic hydrocarbons, which account for about 20–50% of non-methane hydrocarbon emissions in urban areas (Pereira et al., 2015), are considered to be important anthropogenic SOA precursors (Gordon et al., 2014). Briefly, under atmospheric conditions, aromatic species may undergo atmospheric oxidation with ozone (O_3), nitrate (NO_3) and hydroxyl radicals (OH) to form less volatile products which may undergo further reactions, leading to complex chemical composition profiles including a multitude of products. Many chamber and field studies have been conducted to identify SOA constituents and determine SOA yields resulting from the oxidation of aromatic compounds (Forstner et al., 1997; Ng et al., 2007a; Song et al., 2007a; Lu et al., 2009; Pereira et al., 2015; Li et al., 2016). However, comprehensive knowledge of SOA chemical composition and formation mechanisms still remains inadequate due to its complexity and variability in the atmosphere.

In urban environments, benzene, toluene and the xylenes are considered among the most important ambient aromatic hydrocarbons due to their high SOA-forming potentials (Zhou et al., 2011). SOA formed from the oxidation of these aromatic VOCs has been shown to account for 3–25 TgC/yr of SOA production on the global scale (Volkamer et al., 2006). The knowledge on SOA formation from aromatic hydrocarbons under different atmospheric conditions remains incomplete. However, it is clear that anthropogenic SOA in urban environments contributes significantly to the OA mass and can be much higher in concentration than biogenic SOA (Stone et al., 2010; Ding et al., 2012). There are currently few oxidation products suitable for use as tracers of different precursor oxidation systems to assist quantification of contributions to SOA concentrations. Therefore, elucidating and quantifying the oxidation products and their formation pathways, and identification of compounds suitable as tracers of specific precursors remain crucial for understanding SOA formation processes, in the context of their key role in climate change and air quality.

There have been many studies conducted in the past reporting the characterisation of oxidation products and their yields from toluene (Izumi and Fukuyama, 1990; Forstner et al., 1997; Edney et al., 2000; Jang and Kamens, 2001; Volkamer et al., 2001; Ng et al., 2007a; Sato et al., 2007; Arey et al., 2009; Birdsall and Elrod, 2011; Pereira et al., 2015; Chen et al., 2018; Cheng et al., 2021) and *m*-xylene-OH system (Forstner et al., 1997; Zhao et al., 2005; Ng et al., 2007a; Song et al., 2007b; Lu et al., 2009; Birdsall and Elrod, 2011; Li et al., 2018; Zhang et al., 2019). However, the complete determination of SOA products, and their formation pathways under different atmospheric condition were only discussed in a few studies (Forstner et al., 1997; Jang and Kamens, 2001; Zhao et al., 2005; Ng et al., 2007a; Zhang et al., 2019). Most of these studies have only focused on identifying specific class of compounds in the particle or gaseous phase and the detailed speciation was missing. Additionally, some of the oxidation products, known as tracer compounds, can be used in the source apportionment models such as positive matrix factorisation (Srivastava et al., 2018a) and the SOA tracer method (Kleindienst et al., 2007) to estimate the SOA contribution to $PM_{2.5}$ based on observational data. The SOA-tracer method was developed by Kleindienst et al. (2007) to estimate the contributions from biogenic (isoprene, α-pinene, β-caryophyllene) and anthropogenic (toluene) precursors to ambient SOA concentrations using oxidation products as specific or selective tracer compounds. The SOA mass fraction (f_{SOA}) is calculated using the tracer concentrations and the mass of aerosol formed in the smog chamber. The DHOPA (2, 3- dihydroxy 4-oxo pentanoic acid) has been used as a SOA tracer for toluene oxidation in the SOA tracer method (Kleindienst et al., 2007). So far, the DHOPA mass fraction is only available for toluene, however, it may form from other mono aromatics which requires further investigation.

In this context, the present study represents a comprehensive effort to determine in detail the composition of SOA formed from the oxidation of toluene and *m*-xylene. The goals are: (1) to identify particle-phase oxidation products, (2) to assess aromatic oxidation mechanisms, (3) to determine SOA yields, and (4) to estimate the DHOPA mass fraction for toluene and *m*-xylene. To achieve this, a series of laboratory experiments were conducted using a Potential Aerosol Mass (PAM) chamber to generate SOA from toluene and *m*-xylene oxidation with OH under low- and high-NO_x conditions. In addition, we have also tried to estimate yields of both SOA and specific products of these precursors to compare with previously reported values.

2. Materials and methods

2.1. Experimental procedure (PAM)

As shown in Fig. 1, the oxidation experiments of toluene and *m*-xylene under low-NO_x and high-NO_x conditions were conducted in a Potential Aerosol Mass (PAM) oxidation flow reactor (OFR; Aerodyne Research, Inc.). Details on the experimental set up and parameters are provided in the Supporting Information (SI). In this study, the total PAM inlet flowrates for low- and high-NO_x experiments were set to 4.8 L/min, and then the residence time was approximately 166 s. Under low-NO_x conditions, the flow rate of dry air and wet air was 3.1 L/min and 1.4 L/min, respectively and the flow rate of VOCs was 300 mL min^{-1}. The

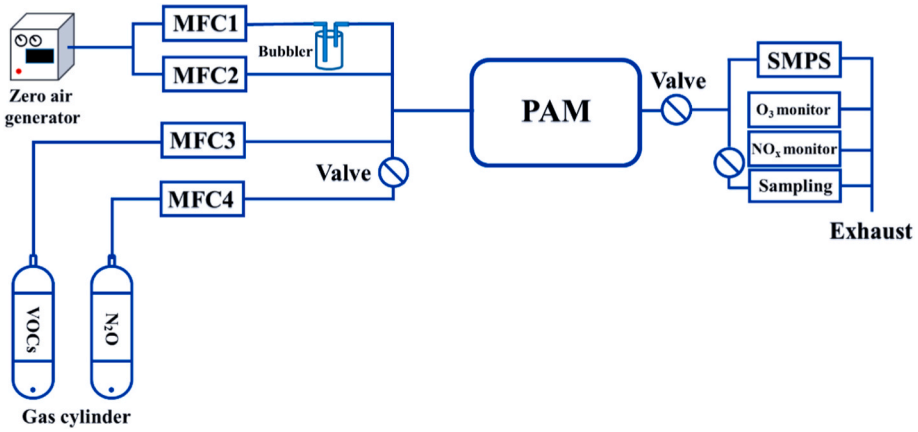

Fig. 1. Experimental setup for toluene and *m*-xylene oxidation with OH radical (MFC: Mass flow controller).

concentration of toluene and *m*-xylene in the gas cylinder was 5.5 and 5.4 ppm, respectively. Under high-NOx condition, the flow rate of dry and wet air was 3.1 L/min and 1.4 L/min while the flow rates of the VOC and N_2O were set to 200 mL min^{-1}, and 190 mL min^{-1} respectively. In these experiments, the 185 mode was used in the PAM. Details on the different PAM operating modes can be found elsewhere (Peng and Jimenez, 2020; Srivastava et al., 2022). Briefly, the UV light used in OFRs typically utilizes either 254 nm ("OFR254") or both 185 and 254 nm ("OFR185") wavelengths. In the OFR185, both 254 and 185 nm photons are available due to the use of clear fused quartz lamps that transmit light of both wavelengths. OH radicals were produced by the photolysis of H_2O, and O_3 was also produced by O_2 photolysis (Lambe et al., 2011). There is no need to add O_3 into the reactor in the 185 mode while the 254 mode requires the external addition of O_3. The voltages of 185 nm and 254 nm lamps were 3 V and 4 V, respectively. When the N_2O was introduced into the PAM, NO and NO_2 are produced via the reaction $O^1D + N_2O \rightarrow 2NO$, followed by the reaction $NO + O_3 \rightarrow NO_2 + O_2$ (Lambe et al., 2017). The sampling flow rate was set to 4 L/min and the density (ρ, g cm^{-3}) of aerosol particles in the SMPS was set to 1.40 g cm^{-3} (Ng et al., 2007b). The mass concentration of the SOA was estimated from the SMPS size distribution. The integrated OH exposure (OH_{exp}, molec cm^{-3} s) is calculated by measuring the decay of a reactive organic species and using the pseudo-first order reaction. Details on the OH_{exp} calculations can be found in the SI. Filters (Pallflex®Tissuquartz™, type: 7202-47 mm) were kept in a refrigerator at −20 °C for analysis. The OH_{exp} was 1.57 × 10^{11} molec cm^{-3} s.

Details on the experiments including reactant concentration, experimental condition (low−/−high NO_x), sampling flow and duration, SOA mass, SOA yields (see section 3.2) and DHOPA mass fraction (see section 3.3) are reported in Table 1.

2.2. Analytical procedure

Extraction procedure: Filter samples were prepared and derivatised following the same procedure as described previously (Srivastava et al., 2018b; Albinet et al., 2019). Briefly, filter punches were extracted with methanol (MeOH, 7 mL) using a sonication technique for 20 min at 25 °C. Two derivatising agents were used and the derivatisation process was performed separately using both agents. The first agent *O*-(2,3,4,5,6,-pentafluorobenzyl)-hydroxylamine (PFBHA) was used for derivatising carbonyl groups (ketones and aldehydes) and the second derivatising agent, N, O-bis(trimethylsilyl) trifluoroacetamide (BSTFA) with 1% trimethyl-chlorosilane (TMCS), was used for alcoholic and acidic OH groups. Both derivatisation processes included the addition of 50 μL of BSTFA and PFBHA to 50 μL of filter extract (1:1) for 30 min and 120 min at 60 °C respectively. Before injection into the GC × GC-TOFMS for analysis, tetradecane-d_{30} was added to the extracts and used as internal standard. The quantification of specific reaction products was made using *cis*-ketopinic acid as a reference standard. In addition, an example of chromatogram (Fig. S1) and the details on the data analysis of the derivatised masses are given in the SI.

GC × GC-TOFMS analysis: Details on the GC × GC-TOFMS analysis can be found elsewhere (Alam et al., 2016). Briefly, filter samples were analysed by a gas chromatograph (7890B, Agilent Technologies), which was interfaced with a Bench TOF-Select, time-of-flight mass spectrometer (Markes International, Llantrisant, UK) using electron impact (EI) ionisation at 70 eV. The initial temperature of the primary oven was held for 3 min at 120 °C then increased at 3 °C/min to 300 °C, followed by 2 °C/min to 330 °C and subsequently held for 3 min. The secondary oven was held at 120 °C for 3 min then ramped to 200 °C at 3 °C/min and held for 3 min, followed by 5 °C/min to 330 °C and subsequently held for 33 min. The transfer line temperature was 325 °C and the ion source temperature was 325 °C. A modulation time of 13 s was used, while a total run time of each sample was 81 min. The separation was performed using the primary (SGE BPX5, 30 m × 0.25 mm ID × 0.25 μm−5% phenyl polysilphenylene-siloxane) and secondary (SGE BPX50, 4.0 m × 0.1 mm ID × 0.1 μm−50% phenyl polysilphenylene-siloxane) columns.

The mass range was 40–600 *m/z* or 40–900 *m/z*, respectively for BSTFA and PFBHA derivatised samples. Data analyses were performed using GC Image v2.3 software (Zoex Corporation, Houston, U.S.A.). Details on the identification of compounds and their characteristic fragment ion peaks are listed in the SI (Tables S1 and S2). In addition, the identifications of compounds were made using the mass spectral data and methodology published previously (Forstner et al., 1997; Edney et al., 2001; Jang and Kamens, 2001; Jaoui et al., 2004; Kleindienst et al., 2004, 2007). In some cases, there is also a possibility of the formation of isomers. These isomers have either the same molecular weight or the same functional groups with different arrangement, which makes their identification difficult. Therefore, it was not always possible to rule out mis-assignments, and this may have resulted in some ambiguous assignments. These compounds are also highlighted in the SI tables.

3. Results

Note, the detailed information on the reaction schemes for toluene-OH (Forstner et al., 1997; Jang and Kamens, 2001) and *m*-xylene-OH (Forstner et al., 1997; Zhao et al., 2005; Zhang et al., 2019) oxidation systems has been published previously. Hence, the full schemes have not been reproduced here. The reaction schemes presented in the current

Table 1
Details on experimental condition and estimated SOA yields for the toluene and xylene oxidation systems.

Reactant	Experimental condition	Sampling flow rate and duration	SOA mass (μg m^{-3})	Yield (%)	f_{SOA} (DHOPA) (current study)	f_{SOA} (DHOPA) Kleindienst et al. (2007)	f_{SOA} (DHOPA) Sato et al. (2022)	f_{SOA} (DHOPA) Al-Naiema et al. (2020)
337 ppb *m*-xylene	low NOx	4L/min 3 h	80	5.0	0.0078	No value	No value	No value
337 ppb *m*-xylene	low NOx	4L/min 3 h	85	5.3	0.0075			
220 ppb *m*-xylene	high NOx	4L/min 2 h	130–150	11.5	0.0061			
273 ppb *m*-xylene	high NOx	4L/min 3 h	130–150	13.2	0.0097			
343 ppb toluene	low NOx	4L/min 3 h	130	9.2	0.0086	0.004 ± 0.0013	0.012	0.0068
343 ppb toluene	low NOx	4L/min 3 h	120	8.5	0.0076			
225 ppb toluene	high NOx	4L/min 2 h	160	11.4	0.0063		0.005	0.0037
225 ppb toluene	high NOx	4L/min 2 h	150	10.7	0.0090			

study are simplified to support the discussion and new findings.

3.1. Oxidation products from toluene

The oxidation products derived from toluene-OH interaction are listed in Tables S1 and S2. In addition, Fig. 2 illustrates the details of the key intermediates and major aromatic and non-aromatic products. Toluene oxidation products are classified into two groups in the SI Tables: ring retaining and ring opening. The formation of benzaldehyde (a), benzoic acid (b), cresol (d) and hydroxy-benzaldehyde (e) are observed under both low- and high-NO_x conditions. In general, OH radical addition onto the aromatic ring under atmospheric conditions is the predominant reaction compared to hydrogen abstraction (Smith et al., 1999; Jang and Kamens, 2001). The oxidation products from methyl groups are formed through H-abstraction, and only observed in the minor abundance. As shown in Fig. 2, benzaldehyde (a) reacts with the OH radical and leads to the formation of benzoic acid (b) via the formation of a peroxy radical. The peroxy radical can react with HO_2 to form the –COOH (carboxylic acid) and O_3 (co-product), or a reaction with NO can lead to the formation of NO_2 and an alkoxy radical (Fig. S2). Note, the reaction of the acylperoxy radical with HO_2 can follow three pathways (Dillon and Crowley, 2008). In addition to the pathway shown, it can also lead to the formation of a peroxy acid and O_2, or an acyloxy radical, O_2 and OH. Dillon and Crowley (2008) demonstrate yields of OH radical from 0.45 to 0.6, so the pathway leading directly to carboxylic acid may be minor. The alkoxy radical further abstracts a hydrogen from another molecule to form a benzoic acid and propagate the radical chain reaction. The reaction of the peroxy radical with HO_2 to form a carboxylic acid is a minor route while the reaction with NO in the polluted environment is the predominant pathway (Orlando and Tyndall, 2012). However, in the current study we suggest the formation of carboxylic acid via reaction with HO_2 as not much NO was available due to excess O_3 present in the system (discussed later). The formation of nitrophenol, methyl nitrophenol, nitrocatechol, methylnitrocatechol and nitrobenzoic acids only occurred under high NO_x conditions while other nitro-aromatics such as hydroxy-nitrobenzaldehyde (m) and hydroxy-nitrobenzoic (n) acid were formed under both conditions. Their formation was linked to a phenoxy radical intermediate (c) formation (via OH addition to the toluene ring), followed by an intermediate reaction with O_2, again with OH and then with NO_2. The reaction of benzoic acid with OH and NO_2 can also lead to the formation of nitrobenzoic acid, although it can only be considered as a minor route due to its dependence upon the formation of benzoic acid via the H-abstraction pathway (Jang and Kamens, 2001). A low abundance of nitro-aromatics was observed under high-NO_x conditions, probably due to the presence of high amounts of O_3 (~30 ppm) that would consume most of the available NO and hence inhibited the reaction of NO and RO_2 and other reactions to form nitro compounds. This was also supported by the measurements conducted during the experiments which reported low levels of NO. Surprisingly, phthalic acid was also identified for both conditions, widely accepted as a SOA tracer from naphthalene (Al-Naiema and Stone, 2017). Phthalic acid formation may occur via a Diels-Alder cycloaddition reaction of furan and maleic anhydride, followed by the dehydration of oxanorbornene dicarboxylic acid anhydride to produce phthalic anhydride (Mahmoud et al., 2014). While such reactions have been successfully demonstrated in the

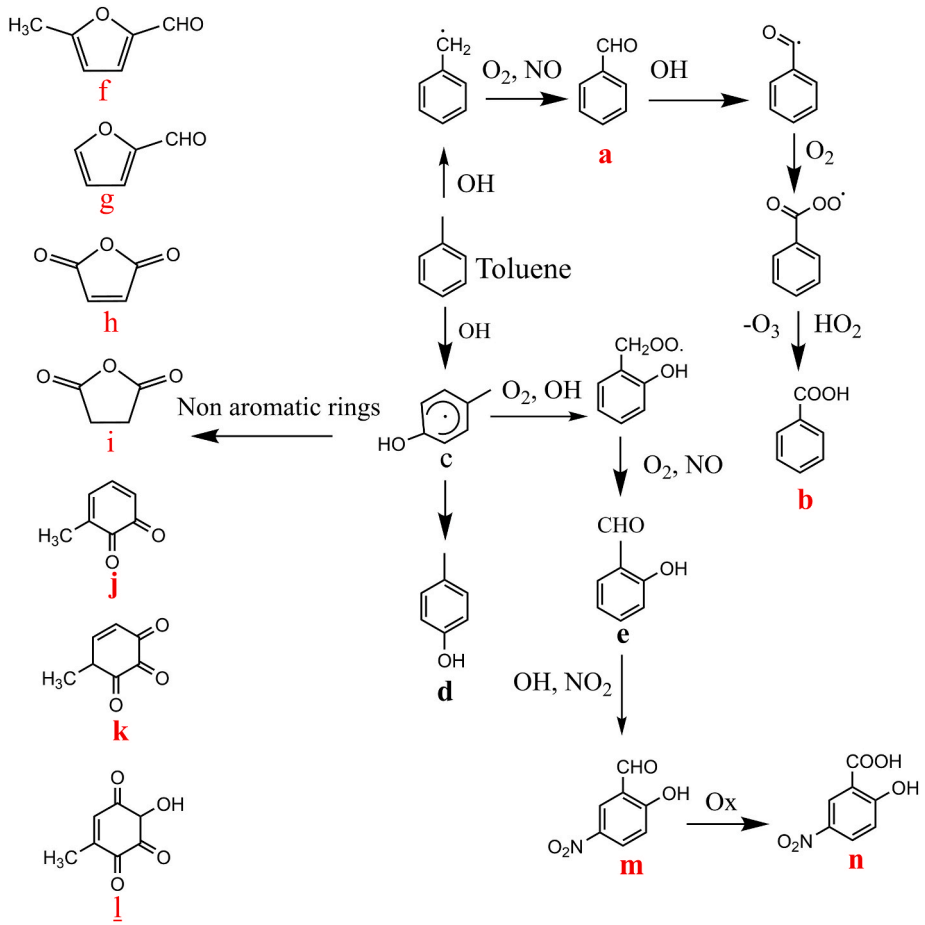

Fig. 2. The key intermediates and the major oxidation products derived from toluene-OH interaction. Colour red: minor compounds, Bold: compounds detected in both low- and high-NO_x, Underline: compounds only detected in high-NO_x. (For interpretation of the references to colour in this figure legend, the reader is referred to the Web version of this article.)

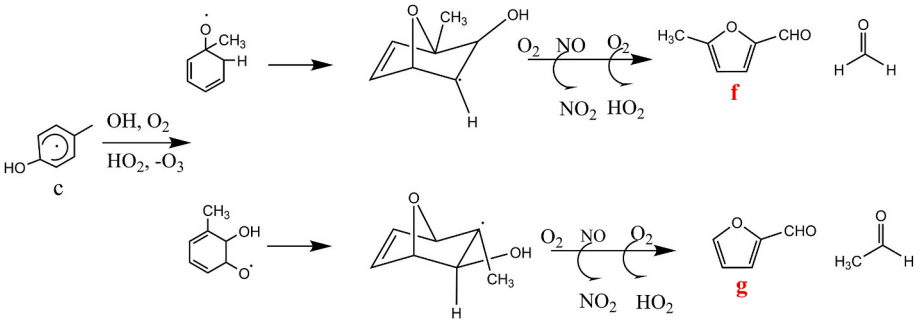

Fig. 3. The key reactions for the formation of furanoid products from toluene-OH interaction. Colour red: minor compounds, Bold: compounds detected in both low- and high-NO_x. (For interpretation of the references to colour in this figure legend, the reader is referred to the Web version of this article.)

laboratory, their occurrence in the atmosphere is still not well established. Note, PAM chamber produces high product concentrations which may enhance the possibility of product-product secondary reactions but probably not relevant to the real environment. However, the current findings indicate a possible role of such reactions in the formation of phthalic acid, and further investigations are necessary to assess their role in the environment.

Small abundance of non-aromatic compounds such as methyl furaldehyde (f), furaldehyde (g), furandione (h), and dihydrofurandione (i) were also observed. Results are consistent with previous studies, as these compounds tend to exist in the gas phase mostly (Forstner et al., 1997; Jang and Kamens, 2001). The formation of methylbenzoquinone (j), and methylcyclohexene tricarbonyls (k) was also observed under both conditions, while hydroxy-methylcyclohexene tricarbonyls (l) were only found under high-NO_x.

Ring retaining non-aromatic products which are formed through epoxy-oxy pathways (Jang and Kamens, 2001; Birdsall and Elrod, 2011), were also observed with significantly smaller intensity, which is consistent with work conducted previously (Li and Wang, 2014; Wu et al., 2014). The formation of furanoid products can occur via a bridged oxide intermediate on a bicyclo ring (Fig. 3) (Shepson et al., 1984). In addition, formation of acyl radical and its reaction with an intra aldehyde group could also leads to furandiones through cyclization (Shepson et al., 1984; Bierbach et al., 1994). Reaction of methylbenzoquinone (j) with OH followed by O_2 and NO may lead to the formation of products such as methylcyclohexene tricarbonyls (k) and

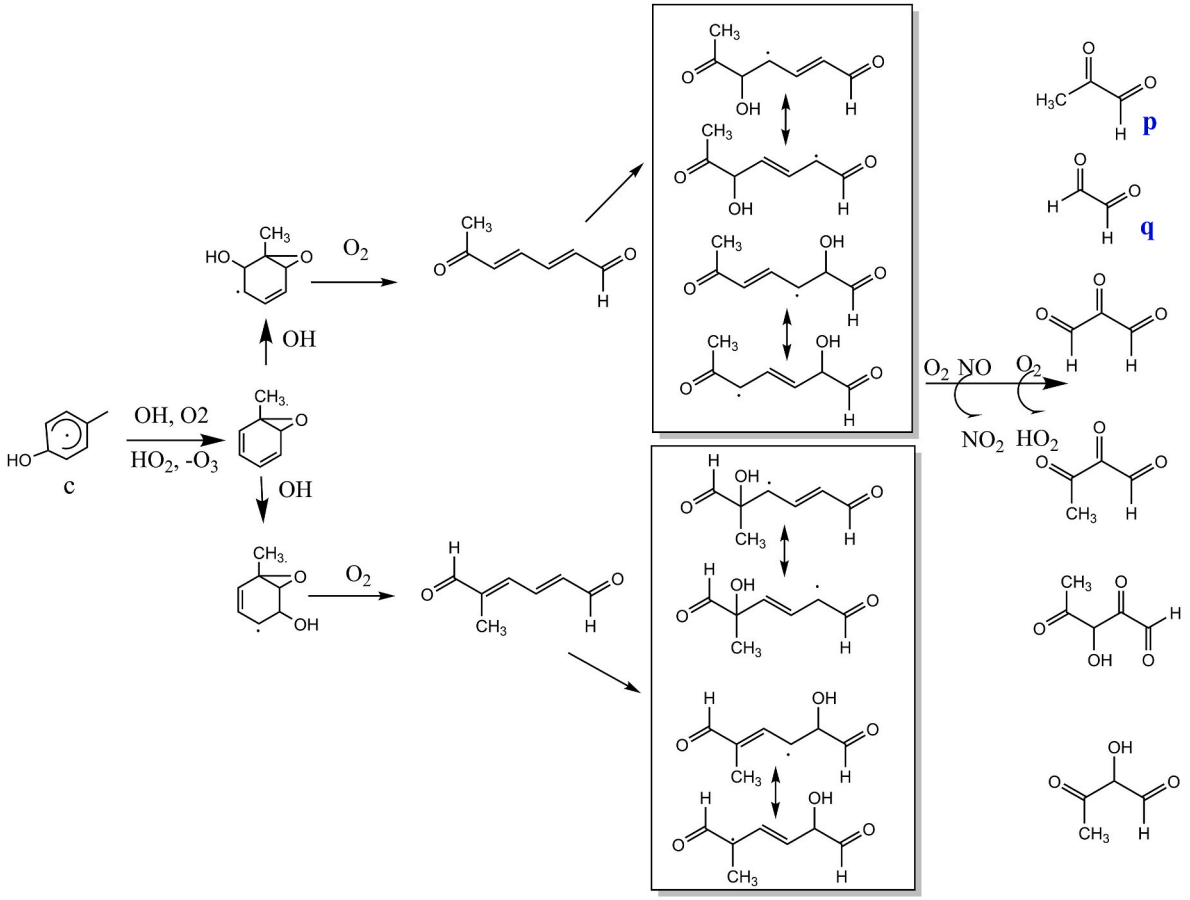

Fig. 4. The key reactions for the formation of ring opening products such methyl glyoxal and glyoxal from toluene-OH interaction. Colour blue: major compounds, Bold: compounds detected in both low- and high-NO_x. (For interpretation of the references to colour in this figure legend, the reader is referred to the Web version of this article.)

hydroxy-methylcyclohexene tricarbonyls (l).

The identified ring opening products included multifunctional oxy-products or oxygenated smaller molecular weight compounds (see Tables S1 and S2). Among the unsaturated dicarbonyls identified, glyoxal (q) and methylglyoxal (p) were the major products. We also observed a high number of compounds containing the –COOH functional group such as such as DHOPA, glyoxalic acid, methyl glyoxalic acid, propanedioic acid, oxo-butenoic acid, oxo-pentenoic acid, succinic acid, oxalic acid, and hydroxy dioxoheptenoic acid. Malic acid was only identified under low-NO_x conditions, while methylhydroxy-oxo-butanedial was only observed during high NO_x experiments. Some other ring-opening products such as hydroxy acetaldehyde, hydroxy hexanal, and dihydroxy propenal were also observed (Tables S1 and S2). Most ring opening products have been formed via phenoxy radical intermediates (c) or the reaction of methylbenzoquinone with OH also including ring opening reactions, which may lead to the formation of highly oxidised multifunctional products. High abundance of glyoxal (q) and methyl glyoxal (p) were observed under both conditions. Their formation pathway may be linked to allylic radical (-C═C–C·) formation via phenoxy radical intermediates, which may undergo isomerization and lead to oxygenated lower molecular weight compounds via carbon-carbon cleavage (Fig. 4) (Jang and Kamens, 2001).

The formation of DHOPA from toluene oxidation has been previously reported in many studies and this compound has been used as a SOA tracer for mono-aromatic compounds (Kleindienst et al., 2007). The formation of DHOPA may occur via the reaction of oxo-pentenal with OH as suggested by Sato et al. (2021). As shown in Fig. 5, the scheme illustrates the formation of 4-oxo-2-pentenal, followed by the reaction with OH and HO_2 in presence of O_2 and NO which lead to the DHOPA formation. The final step of the reaction scheme indicates an addition of HO_2 to an acylperoxy radical to form DHOPA and O_3. However, as noted above, the reaction of HO_2 with the acylperoxy radical can also result in the formation of OH (via cleavage of the weak peroxy bond), but still subsequently leading to the DHOPA formation through H-abstraction by

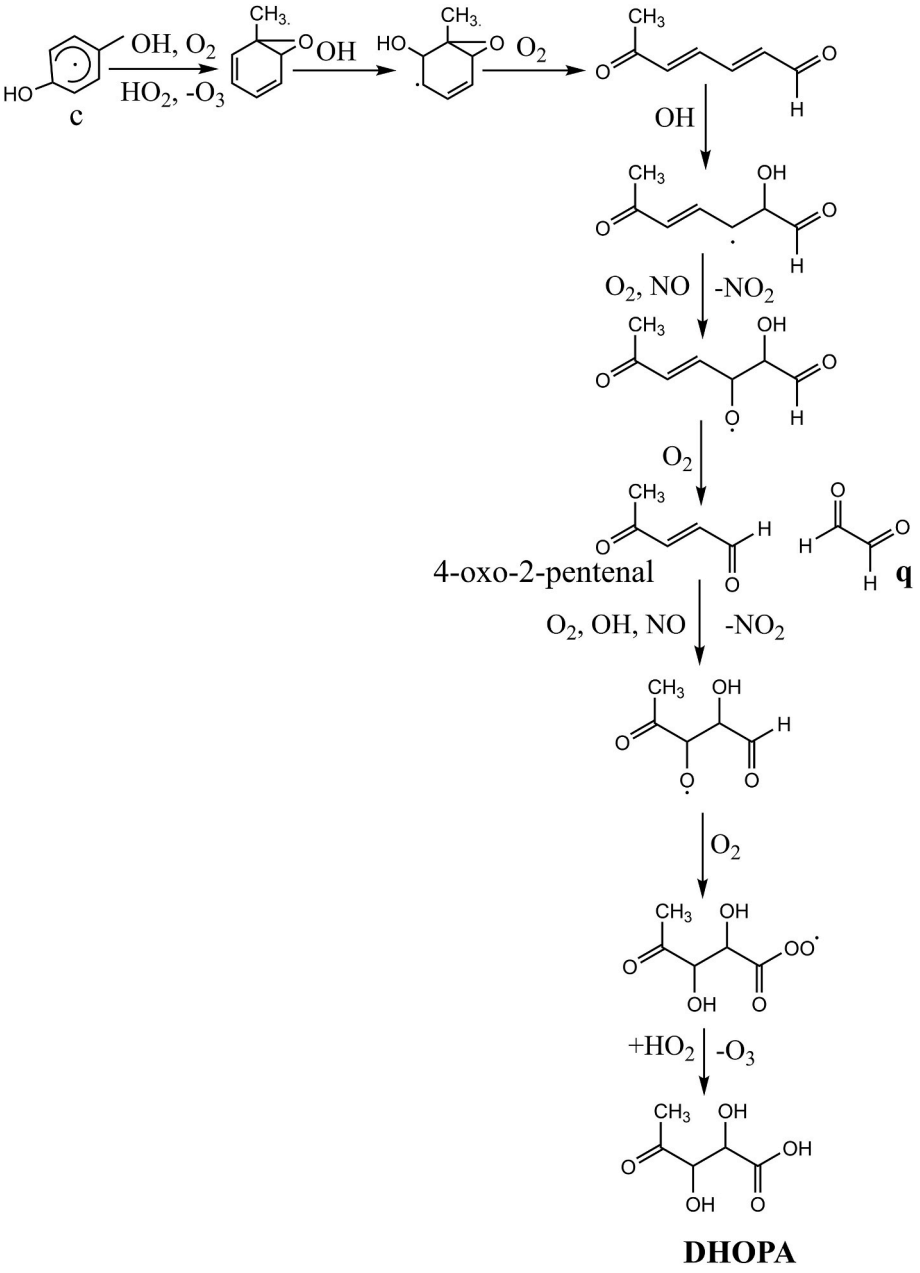

Fig. 5. DHOPA formation from the oxidation of toluene with OH. Bold: compounds detected in both low- and high-NO_x.

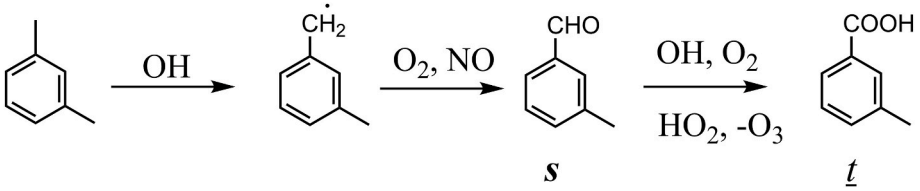

Fig. 6. Proposed mechanism for *m*-toluic acid formation from the oxidation of *m*-xylene. Bold: compounds detected in both low- and high-NO_x, Underline: compounds only detected in high-NO_x.

the resultant acyloxy radical, a pathway which merits further research. In addition, our observation tentatively suggests hydroxy-nitrobenzaldehyde (m) and hydroxy-nitrobenzoic acid (n) could also act as a marker for SOA from toluene oxidation in the atmosphere. Nitro aromatics are also suggested as tracers for anthropogenic SOA by recent field and chamber studies (Ikemori et al., 2019; Sato et al., 2022).

3.2. Oxidation products from xylene

The oxidation products derived from *m*-xylene-OH interaction are listed in Tables S1 and S2. Similar to toluene oxidation, products are classified into two group: ring-retaining and ring-opening. Amongst the ring-retaining aromatic compounds, only tolualdehyde (s) was observed under both low/high-NO_x condition from *m*-xylene oxidation. The formation of *m*-toluic acid (t) and hydroxy-tolualdehyde was only observed under high-NO_x conditions. The pathway leading to *m*-toluic acid (t) and tolualdehyde (s) is similar to the toluene-OH oxidation system, which may be linked to a phenoxy radical intermediate (c) formed via OH addition, followed by an intermediate reaction with O_2/OH/NO (Fig. 6).

Only few nitro-aromatics, such as nitrophenols, methylnitrophenols and methyl nitrocatechols, were observed under high-NO_x via OH addition to the *m*-xylene ring and subsequent reactions with NO. As mentioned, a low abundance of nitro-aromatics from both precursors was attributed to the presence of high O_3 during experiments.

Ring-retaining non-aromatic compounds, such as furaldehyde, methyl furanone, 2, 6 dimethyl-1, 4-benzoquinone, and dihydrofurandione, were observed under both NO_x conditions. In addition, compounds such as furandione, methyl furandione, dimethyl furandione and dimethyl-2H-pyranone were only identified under high-NO_x experiments, which is consistent with previous studies (Forstner et al., 1997; Zhao et al., 2005; Zhang et al., 2019).

The ring-opening compounds included unsaturated ketones, unsaturated aldehydes, as well as organic acids under both conditions. These observations are consistent with the findings reported by Song et al. (2007a) and Birdsall and Elrod (2011), suggesting dicarbonyls comprise a major fraction of ring-opening products from xylene oxidation. The compounds found under both NO_x conditions were: propane triones (C3-triones), glyoxal, methyl glyoxal, oxo-pentenal, 2-methyl-6 oxo 2,4 heptadienal, 2, 3-butanedione, dioxobutanal, dioxo pentanal, hydroxyl acetaldehyde, DHOPA, oxobutenoic acid, oxopentenoic acid, and glyoxalic acid. It has been reported the formation of C3-triones and 2, 3-butadione in SOA formed from xylene oxidation is suppressed under high-NO levels (Zhang et al., 2019). However, this study did not observe

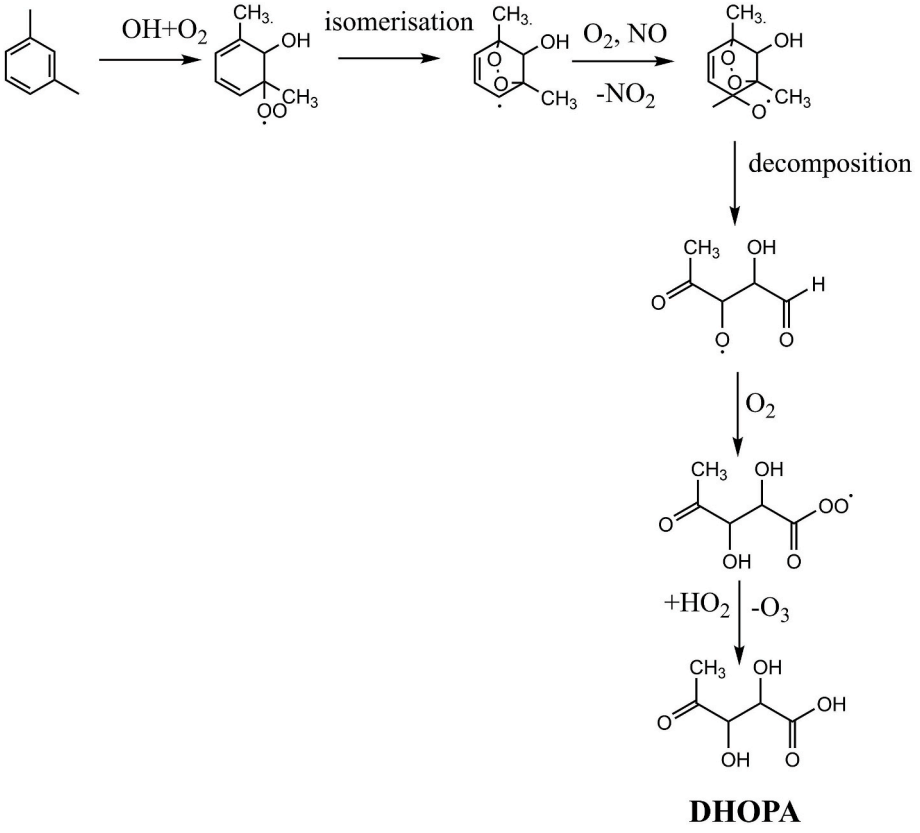

Fig. 7. DHOPA formation from the oxidation of *m*-xylene with OH. Bold: compounds detected in both low- and high-NO_x.

any effect from NO_x levels on the formation of these compounds. Again, NO was likely to be rapidly consumed by O_3 during high NO_x experiments and hence NO levels were significantly reduced later on in the experiments. Glyoxal (u) and methyl glyoxal (v) were found as major products from the xylene-OH reaction, indicating that ring-cleavage pathways involving a bicyclic route play an important role (Volkamer et al., 2001). The bicyclic route involves the formation of secondary peroxy radicals on addition of O_2 which then react with NO to form alkoxy radicals, followed by decomposition to form unsaturated dicarbonyls and subsequently results in the formation of glyoxal (u) or methylglyoxal (v). DHOPA was also observed under both NO_x conditions. Briefly, 4-oxo-2-pentenal as an intermediate plays a major role in the formation of DHOPA. As shown in Fig. 7, 4-oxo-2-pentenal is formed by reactions that include the additions of OH and O_2 to the benzene ring, which then undergoes isomerization, O_2 addition, NO–NO_2 conversion, and decomposition (Wyche et al., 2009). 4-oxo-2-pentenal further reacts with O_2/OH/NO to form a hydroxyalkyloxyl radical, followed by reaction with O_2 and NO–NO_2 conversion. The formed alkoxyl radical can rearrange, add O_2 and HO_2 to give DHOPA. As shown in Fig. 8, another possible alternative pathway for DHOPA could be similar to the toluene-OH oxidation system which may occur via an epoxy intermediate route which results in the formation of methyl glyoxal (v) as a by-product instead of glyoxal (u). However, this pathway has not been confirmed by other studies and needs further investigation. In addition,

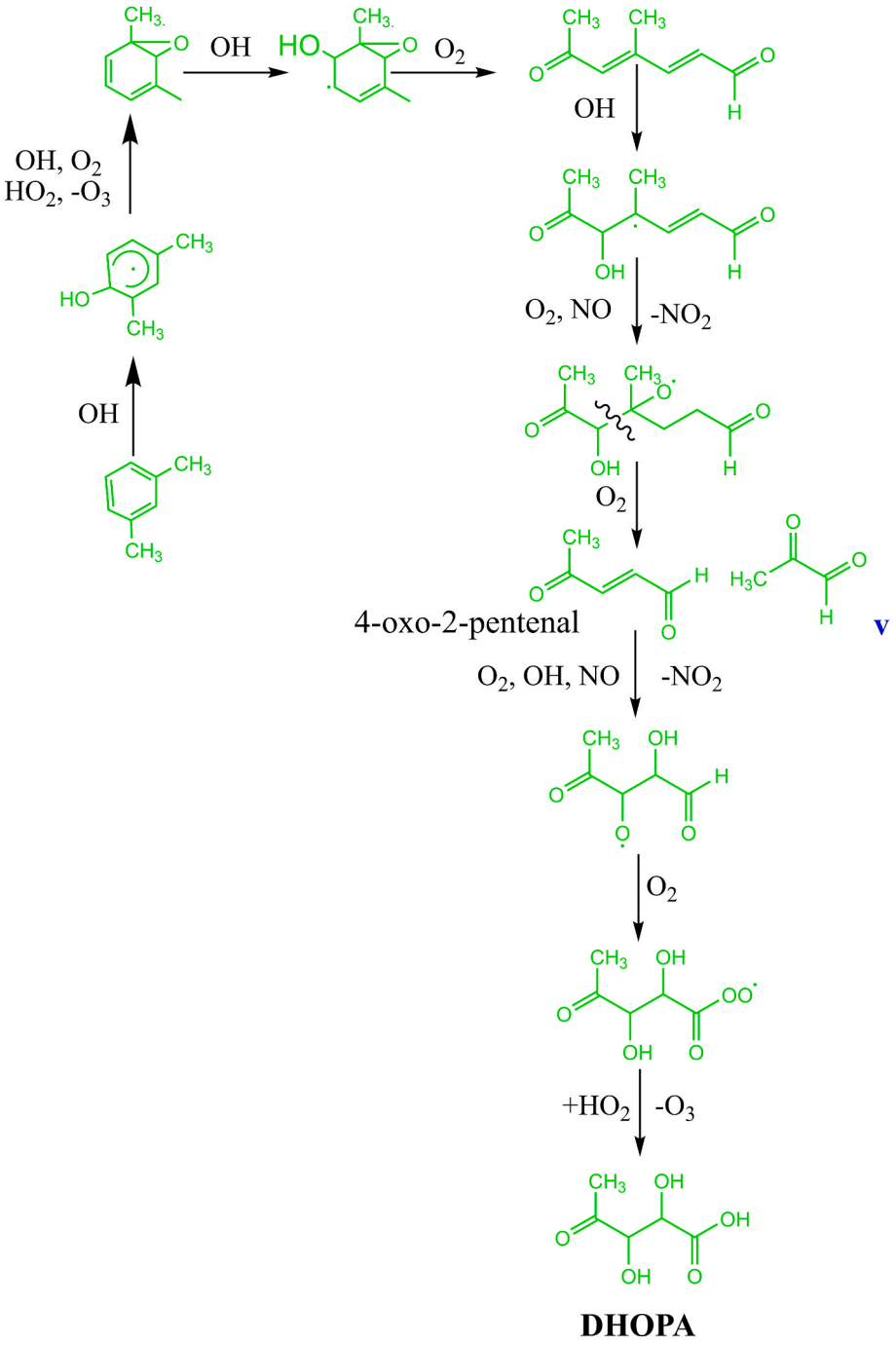

Fig. 8. An alternative pathway (green) for DHOPA formation from the oxidation of *m*-xylene with OH via epoxide intermediate. Colour blue: major compounds, Bold: compounds detected in both low- and high-NO_x. (For interpretation of the references to colour in this figure legend, the reader is referred to the Web version of this article.)

some other ring-opening products were only identified in either condition and are listed in Tables S1 and S2. The current study findings also suggests that the hydroxy-tolualdehyde and *m*-toluic acid, could act as a tracer for the xylene oxidation system in a polluted environment (i.e., high-NO_x).

3.3. SOA yields

The SOA formation potential (i.e., SOA yield) was calculated (see Table 1) and is defined as the ratio of formed SOA mass and the consumed precursor VOCs (Ervens et al., 2011):

$$Y(SOA) = \frac{m(SOA)}{\Delta[VOC]}$$

The average SOA yields for toluene were 0.085, and 0.11 while for *m*-xylene were 0.052 and 0.124 under low- and high-NO_x, respectively. SOA mass was estimated using the SMPS data in the study. Results show that the SOA yields were higher for both precursors under high-NO_x. These results are in contrast to the observations made in previous studies which reported higher SOA yields in low-NOx experiments (Hurley et al., 2001; Ng et al., 2007a). The low-NO_x level promotes O_3 and NO_3 formation that leads to an increase in aerosol formation as these species can subsequently react with both precursor and oxidation products, in addition to the aerosol produced from reaction with the OH itself. However, a lesser SOA yield, as observed here, 0.05–0.053 for toluene and 0.085–0.092 for *m*-xylene may arise due to higher OH concentrations in low-NO_x experiments (OH exposure, low-NO_x: 2.6×10^{12} molec cm^{-3} s, High NO_x: 1.57×10^{11} molec cm^{-3} s). The OH exposure used here were similar to the other PAM studies (Cheng et al., 2021). Some earlier studies have shown a decrease in SOA yield subsequent to an increase in OH exposure, possibly due to breaking of carbon–carbon bonds from continued oxidation, and consequent loss of less volatile reaction products (Lambe et al., 2012; Loza et al., 2012; Hunter et al., 2014).

Both precursors show similar SOA yields under high-NO_x conditions while SOA yields are higher for toluene than those for *m*-xylene under low-NO_x. Ng et al. (2007a) reported higher yields from toluene in a high NO_x, but not in a low-NO_x environment, when using an ammonium nitrate seed aerosol. The higher yields from toluene could be linked to differences in SOA composition as a high number of ring-opening compounds (unsaturated aldehydes, ketones and acids) are produced to a greater extent in the toluene oxidation, leading to higher SOA yields for toluene than for *m*-xylene under low-NO_x. Li et al. (2016) reported that the degree of oxidation decreases with an increase in methyl groups on the aromatic ring. In addition, an increase in SOA yields for *m*-xylene with an increase in VOC concentration was observed (Table 1). An increase in VOC mass concentration could result in an increase in the partitioning into the condensed phase, consequently leading to enhanced SOA yields (Donahue et al., 2006). In our case, this is however based upon only one observation. Note, the particle wall loss correction has not been applied in the present study.

3.4. DHOPA fraction estimation

In the SOA-tracer method, the SOA mass fraction for each precursor, fSOA, is defined as the ratio of the sum of tracer concentrations to the mass concentration of aerosol formed in the smog chamber:

$$f_{SOA} = \frac{\sum Tr_i}{SOA}$$

where Tr_i is the mass concentration of the tracer (μg m^{-3}) and *SOA* is the total mass of aerosol formed in the chamber. In the present study, we have also calculated the DHOPA (*Tr)* mass fraction in SOA for toluene and *m*-xylene precursors (Table 1). The DHOPA mass fractions from toluene and *m*-xylene oxidation were 0.008 ± 0.001 and 0.007 ± 0.001, respectively. The f_{SOA} from toluene oxidation is approximately double that reported previously by Kleindienst et al. (2007) which is given in Table 1. We also observed a similar pattern while comparing to the f_{SOA} value obtained in other studies (Table 1). Note, the tracer concentrations were estimated adopting the same calibration procedure used by Kleindienst et al. (2007). The difference observed in the f_{SOA} could arise from different starting concentrations (~30 times higher precursor concentrations than the current study), experimental conditions (absence of seed aerosols in the current study) or chamber type (PAM vs smog chamber), and possibly even from combined measurement uncertainties. This was also confirmed by the studies conducted previously which reported that the experimental conditions and the use of different types of chambers may affect the composition of formed products (Bruns et al., 2015; Cheng et al., 2021). It is already reported that PAM uses high oxidant concentration to reach high degree of oxygenation compared to the smog chamber (Bruns et al., 2015). The current study used PAM for the oxidation while other studies reported the use of a smog chamber for estimating the DHOPA fraction (Kleindienst et al., 2007; Al-Naiema et al., 2020; Sato et al., 2022) and could cause such a difference. In addition, another recent study (Zhang et al., 2021) reported the modelled f_{SOA} value of 0.002 (estimated using a chemical transport model) which is a factor of 2 and 4 smaller than the value reported previously (Kleindienst et al., 2007) and by the current study. The modeling study also showed a strong dependence of f_{SOA} on the OA loading which further supports the differences observed in the f_{SOA} between the chamber studies. Overall, this suggests the use of DHOPA as a tracer compound is representative of SOA formation from *m*-xylene in addition to toluene. Note, the formation of DHOPA may also occur from xylene isomers (Al-Naiema et al., 2020). This has not been confirmed by the current study and needs further investigation.

4. Conclusion

In this study, we examined the composition of SOA formed during the oxidation of toluene and *m*-xylene with OH radical under low- and high-NO_x conditions. We identified a wide range of oxidation products, including ring-retaining and ring-opening (unsaturated aldehydes, unsaturated ketones and organic acids) compounds. A higher number of ring-opening compounds were observed from toluene oxidation than from *m*-xylene. Glyoxal and methyl glyoxal were the major products from ring-cleavage pathways during the toluene- and *m*-xylene –OH reactions. This indicates that the bicyclic route plays an important role in their formation, which is consistent with observations reported by previous studies. The measured SOA yields were higher for both precursors under high-NO_x than those observed for low-NO_x conditions. This could be attributable to higher OH concentrations during low-NO_x experiments, which may lead to continued oxidation and cleavage of primary oxidation products. In addition, the mass fraction of DHOPA, a known SOA tracer for toluene oxidation products was comparable to (approx. double) that reported previously (Kleindienst et al., 2007). A similar yield of DHOPA was found for *m*-xylene oxidation, indicative of DHOPA formation from oxidation of *m*-xylene other than toluene. Results also suggest an alternative pathway for DHOPA from *m*-xylene oxidation via an epoxy intermediate route, which needs further investigation. This study provides detailed information on oxidation products identified from toluene and *m*-xylene oxidation which can be used to understand their evolution in the atmosphere and consequent impact on health and climate.

Author credit statement

Conceptualization **RMH**, **ZS**; Formal analysis **DS**; Funding acquisition **RMH**, **ZS**; Investigation **DS**; Methodology **ST**, **WL**; Project administration **RMH**, **ZS**; Resources **RMH**, **ZS**; Supervision **RMH**, **ZS**; Validation **RH**, **DS**; Visualization **DS**; Writing – original draft **DS**; Writing – review & editing **ZS**, **ST**, **RMH**.

Declaration of competing interest

The authors declare that they have no known competing financial interests or personal relationships that could have appeared to influence the work reported in this paper.

Data availability

Data will be made available on request.

Acknowledgements

This work was supported by the Natural Environment Research Council (APHH-Beijing and SOA grants): NE/N007190/1 (AIRPOLL-Beijing), NE/S006699/1 (SOA).

Appendix A. Supplementary data

Supplementary data to this article can be found online at https://doi.org/10.1016/j.chemosphere.2023.139002.

References

Al-Naiema, I.M., Offenberg, J.H., Madler, C.J., Lewandowski, M., Kettler, J., Fang, T., Stone, E.A., 2020. Secondary organic aerosols from aromatic hydrocarbons and their contribution to fine particulate matter in Atlanta, Georgia. Atmos. Environ. 223, 1994.

Al-Naiema, I.M., Stone, E.A., 2017. Evaluation of anthropogenic secondary organic aerosol tracers from aromatic hydrocarbons. Atmos. Chem. Phys. 17, 2053–2065.

Alam, M.S., Stark, C., Harrison, R.M., 2016. Using variable ionization energy time-of-flight mass spectrometry with comprehensive GC×GC to identify isomeric species. Anal. Chem. 88, 4211–4220.

Albinet, A., Lanzafame, G.M., Srivastava, D., Bonnaire, N., Nalin, F., Wise, S.A., 2019. Analysis and determination of secondary organic aerosol (SOA) tracers (markers) in particulate matter standard reference material (SRM 1649b, urban dust). Anal. Bioanal. Chem. 411, 5975–5983.

Arey, J., Obermeyer, G., Aschmann, S.M., Chattopadhyay, S., Cusick, R.D., Atkinson, R., 2009. Dicarbonyl products of the OH radical-initiated reaction of a series of aromatic hydrocarbons. Environ. Sci. Technol. 43, 683–689.

Bierbach, A., Barnes, I., Becker, K.H., Wiesen, E., 1994. Atmospheric chemistry of unsaturated carbonyls: butenedial, 4-oxo-2-pentenal, 3-hexene-2, 5-dione, maleic anhydride, 3H-furan-2-one, and 5-methyl-3H-furan-2-one. Environ. Sci. Technol. 28, 715–729.

Birdsall, A.W., Elrod, M.J., 2011. Comprehensive NO-dependent study of the products of the oxidation of atmospherically relevant aromatic compounds. J. Phys. Chem. 115, 5397–5407.

Bruns, E.A., El Haddad, I., Keller, A., Klein, F., Kumar, N.K., Pieber, S.M., Corbin, J.C., Slowik, J.G., Brune, W.H., Baltensperger, U., Prévôt, A.S.H., 2015. Inter-comparison of laboratory smog chamber and flow reactor systems on organic aerosol yield and composition. Atmos. Meas. Tech. 8, 2315–2332.

Chen, Y., Tong, S., Wang, J., Peng, C., Ge, M., Xie, X., Sun, J., 2018. Effect of titanium dioxide on secondary organic aerosol formation. Environ. Sci. Technol. 52, 11612–11620.

Cheng, X., Chen, Q., Jie Li, Y., Zheng, Y., Liao, K., Huang, G., 2021. Highly oxygenated organic molecules produced by the oxidation of benzene and toluene in a wide range of OH exposure and NOx conditions. Atmos. Chem. Phys. 21, 12005–12019.

Daellenbach, K.R., Uzu, G., Jiang, J., Cassagnes, L.-E., Leni, Z., Vlachou, A., Stefenelli, G., Canonaco, F., Weber, S., Segers, A., Kuenen, J.J.P., Schaap, M., Favez, O., Albinet, A., Aksoyoglu, S., Dommen, J., Baltensperger, U., Geiser, M., El Haddad, I., Jaffrezo, J.-L., Prévôt, A.S.H., 2020. Sources of particulate-matter air pollution and its oxidative potential in Europe. Nature 587, 414–419.

Dillon, T.J., Crowley, J.N., 2008. Direct detection of OH formation in the reactions of HO_2 with $CH_3C(O)O_2$ and other substituted peroxy radicals. Atmos. Chem. Phys. 8, 4877–4889.

Ding, X., Wang, X.-M., Gao, B., Fu, X.-X., He, Q.-F., Zhao, X.-Y., Yu, J.-Z., Zheng, M., 2012. Tracer-based estimation of secondary organic carbon in the Pearl River Delta, south China. J. Geophys. Res. 117.

Donahue, N.M., Robinson, A.L., Stanier, C.O., Pandis, S.N., 2006. Coupled partitioning, dilution, and chemical aging of semivolatile organics. Environ. Sci. Technol. 40, 2635–2643.

Edney, E.O., Driscoll, D.J., Speer, R.E., Weathers, W.S., Kleindienst, T.E., Li, W., Smith, D.F., 2000. Impact of aerosol liquid water on secondary organic aerosol yields of irradiated toluene/propylene/NOx/(NH4)2SO4/air mixtures. Atmos. Environ. 34, 3907–3919.

Edney, E.O., Driscoll, D.J., Weathers, W.S., Kleindienst, T.E., Conver, T.S., McIver, C.D., Li, W., 2001. Formation of polyketones in irradiated toluene/propylene/NO_x/air mixtures. Aerosol Sci. Technol. 35, 998–1008.

Ervens, B., Turpin, B.J., Weber, R.J., 2011. Secondary organic aerosol formation in cloud droplets and aqueous particles (aqSOA): a review of laboratory, field and model studies. Atmos. Chem. Phys. 11, 11069–11102.

Forstner, H.J.L., Flagan, R.C., Seinfeld, J.H., 1997. Secondary organic aerosol from the photooxidation of aromatic hydrocarbons: molecular composition. Environ. Sci. Technol. 31, 1345–1358.

Gordon, T.D., Presto, A.A., Nguyen, N.T., Robertson, W.H., Na, K., Sahay, K.N., Zhang, M., Maddox, C., Rieger, P., Chattopadhyay, S., Maldonado, H., Maricq, M.M., Robinson, A.L., 2014. Secondary organic aerosol production from diesel vehicle exhaust: impact of aftertreatment, fuel chemistry and driving cycle. Atmos. Chem. Phys. 14, 4643–4659.

Hunter, J.F., Carrasquillo, A.J., Daumit, K.E., Kroll, J.H., 2014. Secondary organic aerosol formation from acyclic, monocyclic, and polycyclic alkanes. Environ. Sci. Technol. 48, 10227–10234.

Hurley, M.D., Sokolov, O., Wallington, T.J., Takekawa, H., Karasawa, M., Klotz, B., Barnes, I., Becker, K.H., 2001. Organic aerosol formation during the atmospheric degradation of toluene. Environ. Sci. Technol. 35, 1358–1366.

Ikemori, F., Nakayama, T., Hasegawa, H., 2019. Characterization and possible sources of nitrated mono- and di-aromatic hydrocarbons containing hydroxyl and/or carboxyl functional groups in ambient particles in Nagoya. Japan. Atmos. Environ. 211, 91–102.

Izumi, K., Fukuyama, T., 1990. Photochemical aerosol formation from aromatic hydrocarbons in the presence of NOx. Atmos. Environ. 24, 1433–1441.

Jang, M., Kamens, R.M., 2001. Characterization of secondary aerosol from the photooxidation of toluene in the presence of NOx and 1-propene. Environ. Sci. Technol. 35, 3626–3639.

Jaoui, M., Kleindienst, T.E., Lewandowski, M., Edney, E.O., 2004. Identification and quantification of aerosol polar oxygenated compounds bearing carboxylic or hydroxyl groups. 1. Method Dev.. Anal. Chem. 76, 4765–4778.

Kleindienst, T., Conver, T., McIver, C., Edney, E., 2004. Determination of secondary organic aerosol products from the photooxidation of toluene and their implications in ambient PM2. 5. J. Atmos. Chem. 47, 79–100.

Kleindienst, T.E., Jaoui, M., Lewandowski, M., Offenberg, J.H., Lewis, C.W., Bhave, P.V., Edney, E.O., 2007. Estimates of the contributions of biogenic and anthropogenic hydrocarbons to secondary organic aerosol at a southeastern US location. Atmos. Environ. 41, 8288–8300.

Lambe, A., Massoli, P., Zhang, X., Canagaratna, M., Nowak, J., Daube, C., Yan, C., Nie, W., Onasch, T., Jayne, J., Kolb, C., Davidovits, P., Worsnop, D., Brune, W., 2017. Controlled nitric oxide production via O(1D) + N2O reactions for use in oxidation flow reactor studies. Atmos. Meas. Tech. 10, 2283–2298.

Lambe, A.T., Ahern, A.T., Williams, L.R., Slowik, J.G., Wong, J.P.S., Abbatt, J.P.D., Brune, W.H., Ng, N.L., Wright, J.P., Croasdale, D.R., Worsnop, D.R., Davidovits, P., Onasch, T.B., 2011. Characterization of aerosol photooxidation flow reactors: heterogeneous oxidation, secondary organic aerosol formation and cloud condensation nuclei activity measurements. Atmos. Meas. Tech. 4, 445–461.

Lambe, A.T., Onasch, T.B., Croasdale, D.R., Wright, J.P., Martin, A.T., Franklin, J.P., Massoli, P., Kroll, J.H., Canagaratna, M.R., Brune, W.H., Worsnop, D.R., Davidovits, P., 2012. Transitions from functionalization to fragmentation reactions of laboratory secondary organic aerosol (SOA) generated from the OH oxidation of alkane precursors. Environ. Sci. Technol. 46, 5430–5437.

Li, K., Li, J., Wang, W., Li, J., Peng, C., Wang, D., Ge, M., 2018. Effects of gas-particle partitioning on refractive index and chemical composition of *m*-xylene secondary organic aerosol. J. Phys. Chem. 122, 3250–3260.

Li, L., Tang, P., Nakao, S., Chen, C.L., Cocker Iii, D.R., 2016. Role of methyl group number on SOA formation from monocyclic aromatic hydrocarbons photooxidation under low-NOx conditions. Atmos. Chem. Phys. 16, 2255–2272.

Li, Y., Wang, L., 2014. The atmospheric oxidation mechanism of 1, 2, 4-trimethylbenzene initiated by OH radicals. Phys. Chem. Chem. Phys. 16, 17908–17917.

Loza, C.L., Chhabra, P.S., Yee, L.D., Craven, J.S., Flagan, R.C., Seinfeld, J.H., 2012. Chemical aging of m-xylene secondary organic aerosol: laboratory chamber study. Atmos. Chem. Phys. 12, 151–167.

Lu, Z., Hao, J., Takekawa, H., Hu, L., Li, J., 2009. Effect of high concentrations of inorganic seed aerosols on secondary organic aerosol formation in the m-xylene/NOx photooxidation system. Atmos. Environ. 43, 897–904.

Mahmoud, E., Watson, D.A., Lobo, R.F., 2014. Renewable production of phthalic anhydride from biomass-derived furan and maleic anhydride. Green Chem. 16, 167–175.

Ng, N., Kroll, J., Chan, A., Chhabra, P., Flagan, R., Seinfeld, J., 2007a. Secondary organic aerosol formation from m-xylene, toluene, and benzene. Atmos. Chem. Phys. 7, 3909–3922.

Ng, N.L., Chhabra, P.S., Chan, A.W.H., Surratt, J.D., Kroll, J.H., Kwan, A.J., McCabe, D. C., Wennberg, P.O., Sorooshian, A., Murphy, S.M., Dalleska, N.F., Flagan, R.C., Seinfeld, J.H., 2007b. Effect of NO_x level on secondary organic aerosol (SOA) formation from the photooxidation of terpenes. Atmos. Chem. Phys. 7, 5159–5174.

Orlando, J.J., Tyndall, G.S., 2012. Laboratory studies of organic peroxy radical chemistry: an overview with emphasis on recent issues of atmospheric significance. Chem. Soc. Rev. 41, 6294–6317.

Peng, Z., Jimenez, J.L., 2020. Radical chemistry in oxidation flow reactors for atmospheric chemistry research. Chem. Soc. Rev. 49, 2570–2616.

Pereira, K.L., Hamilton, J.F., Rickard, A.R., Bloss, W.J., Alam, M.S., Camredon, M., Ward, M.W., Wyche, K.P., Muñoz, A., Vera, T., Vázquez, M., Borrás, E., Ródenas, M., 2015. Insights into the formation and evolution of individual compounds in the particulate phase during aromatic photo-oxidation. Environ. Sci. Technol. 49, 13168–13178.

Sato, K., Hatakeyama, S., Imamura, T., 2007. Secondary organic aerosol formation during the photooxidation of toluene: NOx dependence of chemical composition. J. Phys. Chem. 111, 9796–9808.

Sato, K., Ikemori, F., Ramasamy, S., Fushimi, A., Kumagai, K., Iijima, A., Morino, Y., 2021. Four- and five-carbon dicarboxylic acids present in secondary organic aerosol produced from anthropogenic and biogenic volatile organic compounds. Atmos 12, 1703.

Sato, K., Ikemori, F., Ramasamy, S., Iijima, A., Kumagai, K., Fushimi, A., Fujitani, Y., Chatani, S., Tanabe, K., Takami, A., Tago, H., Saito, Y., Saito, S., Hoshi, J., Morino, Y., 2022. Formation of secondary organic aerosol tracers from anthropogenic and biogenic volatile organic compounds under varied NOx and oxidant conditions. Atmos. Environ. 14, 100169.

Shepson, P.B., Edney, E.O., Corse, E.W., 1984. Ring fragmentation reactions in the photooxidations of toluene and o-xylene. J. Phys. Chem. 88, 4122–4126.

Smith, D.F., Kleindienst, T.E., McIver, C.D., 1999. Primary product distributions from the reaction of OH with m-, p-xylene, 1,2,4- and 1,3,5-trimethylbenzene. J. Atmos. Chem. 34, 339–364.

Song, C., Na, K., Warren, B., Malloy, Q., Cocker, D.R., 2007a. Secondary organic aerosol formation from the photooxidation of p- and o-xylene. Environ. Sci. Technol. 41, 7403–7408.

Song, C., Na, K., Warren, B., Malloy, Q., Cocker 3rd, D.R., 2007b. Secondary organic aerosol formation from m-xylene in the absence of NOx. Environ. Sci. Technol. 41, 7409–7416.

Srivastava, D., Favez, O., Bonnaire, N., Lucarelli, F., Perraudin, E., Gros, V., Villenave, E., Albinet, A., 2018a. Speciation of organic fractions does matter for aerosol source apportionment. Part 2: intensive campaign in the Paris area (France). Sci. Total Environ. 634, 267–278.

Srivastava, D., Tomaz, S., Favez, O., Lanzafame, G.M., Golly, B., Besombes, J.L., Alleman, L.Y., Jaffrezo, J.L., Jacob, V., Perraudin, E., Villenave, E., Albinet, A., 2018b. Speciation of organic fraction does matter for source apportionment. Part 1: a one-year campaign in Grenoble (France). Sci. Total Environ. 624, 1598–1611.

Srivastava, D., Vu, T.V., Tong, S., Shi, Z., Harrison, R.M., 2022. Formation of secondary organic aerosols from anthropogenic precursors in laboratory studies. npj Clim. Atmos. Sci. 5, 22.

Stone, E.A., Hedman, C.J., Zhou, J., Mieritz, M., Schauer, J.J., 2010. Insights into the nature of secondary organic aerosol in Mexico City during the MILAGRO experiment 2006. Atmos. Environ. 44, 312–319.

Volkamer, R., Jimenez, J.L., San Martini, F., Dzepina, K., Zhang, Q., Salcedo, D., Molina, L.T., Worsnop, D.R., Molina, M.J., 2006. Secondary organic aerosol formation from anthropogenic air pollution: rapid and higher than expected. Geophys. Res. Lett. 33.

Volkamer, R., Platt, U., Wirtz, K., 2001. Primary and secondary glyoxal formation from aromatics: experimental evidence for the Bicycloalkyl−Radical pathway from benzene, toluene, and p-xylene. J. Phys. Chem. 105, 7865–7874.

Wu, R., Pan, S., Li, Y., Wang, L.J.T.J.o.P.C.A., 2014. Atmospheric oxidation mechanism of toluene. J. Phys. Chem. 118, 4533–4547.

Wyche, K.P., Monks, P.S., Ellis, A.M., Cordell, R.L., Parker, A.E., Whyte, C., Metzger, A., Dommen, J., Duplissy, J., Prevot, A.S.H., Baltensperger, U., Rickard, A.R., Wulfert, F., 2009. Gas phase precursors to anthropogenic secondary organic aerosol: detailed observations of 1,3,5-trimethylbenzene photooxidation. Atmos. Chem. Phys. 9, 635–665.

Zhang, J., He, X., Gao, Y., Zhu, S., Jing, S., Wang, H., Yu, J.Z., Ying, Q., 2021. Estimation of aromatic secondary organic aerosol using a molecular tracer—a chemical transport model assessment. Environ. Sci. Technol. 55, 12882–12892.

Zhang, P., Huang, J., Shu, J., Yang, B., 2019. Comparison of secondary organic aerosol (SOA) formation during o-, m-, and p-xylene photooxidation. Environ. Pollut. 245, 20–28.

Zhao, J., Zhang, R., Misawa, K., Shibuya, K., 2005. Experimental product study of the OH-initiated oxidation of m-xylene. J. Photochem. Photobiol. A-Chem. 176, 199–207.

Zhou, Y., Zhang, H., Parikh, H.M., Chen, E.H., Rattanavaraha, W., Rosen, E.P., Wang, W., Kamens, R.M., 2011. Secondary organic aerosol formation from xylenes and mixtures of toluene and xylenes in an atmospheric urban hydrocarbon mixture: water and particle seed effects (II). Atmos. Environ. 45, 3882–3890.